JAMA Neurology | Original Investigation

Increased Medial Temporal Tau Positron Emission Tomography Uptake in the Absence of Amyloid-β Positivity

Alejandro Costoya-Sánchez, MSc; Alexis Moscoso, PhD; Jesús Silva-Rodríguez, PhD; Michael J. Pontecorvo, PhD; Michael D. Devous Sr, PhD; Pablo Aguiar, PhD; Michael Schöll, PhD; Michel J. Grothe, PhD; for the Alzheimer's Disease Neuroimaging Initiative and the Harvard Aging Brain Study

IMPORTANCE An increased tau positron emission tomography (PET) signal in the medial temporal lobe (MTL) has been observed in older individuals in the absence of amyloid-β (Aβ) pathology. Little is known about the longitudinal course of this condition, and its association with Alzheimer disease (AD) remains unclear.

OBJECTIVE To study the pathologic and clinical course of older individuals with PET-evidenced MTL tau deposition ($TMTL^+$) in the absence of Aβ pathology (A^-), and the association of this condition with the AD continuum.

DESIGN, SETTING, AND PARTICIPANTS A multicentric, observational, longitudinal cohort study was conducted using pooled data from the Alzheimer's Disease Neuroimaging Initiative (ADNI), Harvard Aging Brain Study (HABS), and the AVID-A05 study, collected between July 2, 2015, and August 23, 2021. Participants in the ADNI, HABS, and AVID-A05 studies (N = 1093) with varying degrees of cognitive performance were deemed eligible if they had available tau PET, Aβ PET, and magnetic resonance imaging scans at baseline. Of these, 128 participants did not meet inclusion criteria based on Aβ PET and tau PET biomarker profiles (A^+ $TMTL^-$).

EXPOSURES Tau and Aβ PET, magnetic resonance imaging, cerebrospinal fluid biomarkers, and cognitive assessments.

MAIN OUTCOMES AND MEASURES Cross-sectional and longitudinal measures for tau and Aβ PET, cortical atrophy, cognitive scores, and core AD cerebrospinal fluid biomarkers (Aβ42/40 and tau phosphorylated at threonine 181 p-tau181 available in a subset).

RESULTS Among the 965 individuals included in the study, 503 were women (52.1%) and the mean (SD) age was 73.9 (8.1) years. A total of 51% of A^- individuals and 78% of A^+ participants had increased tau PET signal in the entorhinal cortex ($TMTL^+$) compared with healthy younger (aged <39 years) controls. Compared with A^- $TMTL^-$, A^- $TMTL^+$ participants showed statistically significant, albeit moderate, longitudinal (mean [SD], 1.83 [0.84] years) tau PET increases that were largely limited to the temporal lobe, whereas those with A^+ $TMTL^+$ showed faster and more cortically widespread tau PET increases. In contrast to participants with A^+ $TMTL^+$, those with A^- $TMTL^+$ did not show any noticeable Aβ accumulation over follow-up (mean [SD], 2.36 [0.76] years). Complementary cerebrospinal fluid analysis confirmed longitudinal p-tau181 increases in A^- $TMTL^+$ in the absence of increased Aβ accumulation. Participants with A^- $TMTL^+$ had accelerated MTL atrophy, whereas those with A^+ $TMTL^+$ showed accelerated atrophy in widespread temporoparietal brain regions. Increased MTL tau PET uptake in A^- individuals was associated with cognitive decline, but at a significantly slower rate compared with A^+ $TMTL^+$.

CONCLUSIONS AND RELEVANCE In this study, individuals with A^- $TMTL^+$ exhibited progressive tau accumulation and neurodegeneration, but these processes were comparably slow, remained largely restricted to the MTL, were associated with only subtle changes in global cognitive performance, and were not accompanied by detectable accumulation of Aβ biomarkers. These data suggest that individuals with A^- $TMTL^+$ are not on a pathologic trajectory toward AD.

JAMA Neurol. doi:10.1001/jamaneurol.2023.2560
Published online August 14, 2023.

Editorial
Supplemental content

Author Affiliations: Author affiliations are listed at the end of this article.

Group Information: Members of the Alzheimer's Disease Neuroimaging Initiative and the Harvard Aging Brain Study appear in Supplement 2.

Corresponding Authors: Michel J. Grothe, PhD, Unidad de Trastornos del Movimiento, Instituto de Biomedicina de Sevilla (IBiS), Campus Hospital Universitario Virgen del Rocío, Avda. Manuel Siurot, s/n, 41013 Sevilla, Spain (mgrothe@us.es); Michael Schöll, PhD, Sahlgrenska University Hospital, Wallinsgatan 6, 43141 Mölndal, Sweden (michael.scholl@neuro.gu.se).

Amyloid-β (Aβ) plaques and tau neurofibrillary tangles are the hallmarks of Alzheimer disease (AD).[1,2] The presence of neurofibrillary tangles has been observed to be tightly linked to increased Aβ load.[3] However, the presence of neurofibrillary tangles in the medial temporal lobe (MTL) has also been observed in older individuals without substantial Aβ pathology,[4] a condition that has been termed *primary age-related tauopathy* (PART).[5] Over recent years, clinicopathologic association studies have shed light on the clinical and neurodegenerative correlates of PART.[6-10] Yet, being a neuropathologic entity that is only diagnosed at autopsy, little is known about the temporal course of this condition, and its association with downstream Aβ accumulation and the AD continuum[11] remains controversial.[12-14]

Positron emission tomography (PET) studies have also consistently shown increased MTL tau PET signal in a subset of individuals with negative Aβ PET scans,[15-17] which may reflect PART, among other possible conditions.[18] The in vivo PET-based identification of these individuals also allows studying their future clinical and pathologic progression.

In this study, we used data from a large multicohort sample to study the longitudinal pathologic characteristics and future clinical course of Aβ PET-negative (A^-) individuals who show increased MTL tau PET signal ($TMTL^+$). Specifically, we studied baseline characteristics and longitudinal changes in cognition, neuroimaging, and cerebrospinal fluid (CSF) biomarkers in these individuals and contrasted them to biomarker-negative controls as well as to individuals with an AD-typical Aβ- and tau-positive PET profile.

Key Points

Question What is the longitudinal trajectory of older individuals who show positron emission tomography–assessed medial temporal lobe (MTL) tau deposition in the absence of amyloid-β (Aβ) pathology (A^- $TMTL^+$)?

Findings In this cohort study of 969 older participants, A^- $TMTL^+$ individuals displayed moderate tau accumulation mainly restricted to the MTL, which was paralleled by cerebrospinal fluid phosphorylated tau increases and colocalized atrophy progression; no significant Aβ accumulation was observed. By contrast, Aβ-positive individuals showed pronounced and cortically widespread tau accumulation, which was accompanied by extratemporal cortical atrophy and significantly faster cognitive decline.

Meaning The findings of this study suggest that individuals with A^- $TMTL^+$ do not appear to be on a pathologic trajectory toward Alzheimer disease.

Methods

Study Design

Data used in the preparation of this article were obtained from the Alzheimer's Disease Neuroimaging Initiative (ADNI), Harvard Aging Brain Study (HABS),[19] and AVID-A05 study cohorts (eMethods in Supplement 1). Informed written consent was obtained from all participants or their corresponding caregivers. All protocols were approved by each cohort's respective institutional ethical review board. This study followed the Strengthening the Reporting of Observational Studies in Epidemiology (STROBE) reporting guideline. Data were collected between July 2, 2015, and August 23, 2021. We included all participants who had undergone concurrent structural magnetic resonance imaging, Aβ PET, tau PET, and clinical evaluation within a 6-month window (N = 1093). Participants were further classified into 4 groups according to PET-based Aβ (A) and tau (T) status, as described in the Neuroimaging section: A^- $TMTL^-$ (n = 250), A^- $TMTL^+$ (n = 264), A^+ $TMTL^+$ (n = 451), and A^+ $TMTL^-$ (n = 128). Additionally, a subcohort of 16 healthy younger controls (maximum age, <39 years) with concurrent magnetic resonance imaging and tau PET scans from the AVID-A05 study was included for the definition of the tau PET positivity threshold.

A subset from the ADNI study had baseline and follow-up CSF biomarkers available (described in the CSF Biomarkers section), and all participants had baseline cognitive data. Subsets of the study participants underwent follow-up neuroimaging (mean [SD], 2.36 [0.76] years for Aβ PET and 1.83 [0.84] years for tau PET) and cognitive assessments (eMethods in Supplement 1). Participants' characteristics are provided in the **Table**.

Neuroimaging

Magnetic resonance imaging acquisition details for ADNI, HABS, and AVID-A05 are reported in the eMethods in Supplement 1. Magnetic resonance images were segmented with FreeSurfer, version 7.1.1 and Statistical Parametric Mapping 12 (SPM12, Wellcome Department of Imaging Neuroscience, Institute of Neurology). FreeSurfer-derived regions of interest (ROI) were merged to generate masks resembling regions affected by neurofibrillary tangle pathology in Braak stages I/II, III/IV, and V/VI (eMethods in Supplement 1).[20,21] FreeSurfer-based cortical thickness maps were coregistered to the fsaverage template and smoothed with a 2-dimensional isotropic gaussian filter of 12 mm full width at half maximum.

PET acquisitions followed study-specific protocols that are detailed in the eMethods in Supplement 1. Tau-PET scans were acquired using [^{18}F]flortaucipir (FTP), and Aβ-PET scans were acquired using either [^{18}F]florbetapir (ADNI and AVID-A05), [^{18}F]florbetaben (ADNI), or [^{11}C]Pittsburgh compound B (HABS) radiotracers. The multicentric PET scans were preprocessed using an in-house-developed pipeline that replicated the ADNI pipeline for PET scanner harmonization.[22,23] Scanner-specific gaussian filters were applied to each PET image (regardless of PET imaging modality) to reach a uniform isotropic resolution of 8 mm.

For FTP-PET scans, region-based voxelwise[24] partial volume correction was applied using the PETPVC toolbox[25] and Baker atlas.[26] Global standardized uptake value ratio (SUVR) in Aβ-PET scans was quantified using the centiloid scale[27] (eMethods in Supplement 1). In addition, cortical surface SUVR maps were generated for all PET scans using FreeSurfer,[28,29] coregistered to the fsaverage template, and smoothed with a 2-dimensional isotropic gaussian filter of 10 mm full width at half maximum.

Table. Cohort Characteristics

Characteristic	A^- $TMTL^-$ (n = 250)	A^- $TMTL^+$ (n = 264)	A^+ $TMTL^+$ (n = 451)
Study, No. (%)			
ADNI	128 (51.2)	178 (67.4)	330 (73.2)
HABS	65 (26.0)	52 (19.7)	36 (8.0)
AVID-A05	57 (22.8)	34 (12.9)	85 (18.8)
Age, mean (SD), y	70.0 (7.8)	74.9 (7.6)	75.6 (8.0)
Gender, No. (%)			
Men	108 (43.2)	133 (50.4)	221 (49.0)
Women	142 (56.8)	131 (49.6)	230 (51.0)
Years of education, mean (SD)	15.96 (2.80)	16.73 (2.60)	16.43 (2.47)
APOE-ε4 carrier, No. (%)[a]	49 (19.9)	45 (18.0)	236 (54.4)
APOE-ε2 carrier, No. (%)[a]	42 (16.3)	36 (14.4)	19 (4.4)
Cognitive status, No. (%)			
CU	189 (75.6)	175 (66.3)	180 (39.9)
MCI	55 (22.0)	71 (26.9)	172 (38.1)
ADD	6 (2.4)	18 (6.8)	99 (22.0)
MMSE score, mean (SD)	28.9 (1.59)	28.6 (1.93)	26.9 (3.60)
CU PACC-3, mean (SD)	0.25 (1.92)	−0.17 (2.30)	−0.27 (2.23)
CI ADAS-Cog 11, mean (SD)	9.85 (5.50)	10.3 (5.4)	13.9 (7.4)
Baseline biomarkers, mean (SD)			
Centiloids	−0.72 (7.76)	0.46 (7.89)	68.52 (37.31)
Braak stages I/II FTP SUVR	1.10 (0.09)	1.42 (0.35)	1.80 (0.56)
Braak stages III/IV FTP SUVR	1.19 (0.08)	1.30 (0.11)	1.72 (0.67)
Braak stages V/VI FTP SUVR	1.07 (0.08)	1.15 (0.10)	1.37 (0.44)
Log CSF Aβ42/40	−2.47 (0.19)	−2.50 (0.22)	−3.20 (0.41)
Log CSF p-tau181, pg/mL	2.80 (0.32)	2.91 (0.31)	3.32 (0.47)
Longitudinal biomarkers and cognition, yearly rates of change (SE)			
Centiloids	−0.17 (0.55)	0.0132 (0.6)	3.04 (1.98)
Braak stages I/II FTP SUVR	0.01 (0.02)	0.02 (0.02)	0.06 (0.05)
Braak stages III/IV FTP SUVR	0.01 (0.01)	0.02 (0.01)	0.07 (0.07)
Braak stages V/VI FTP SUVR	0.01 (0.01)	0.01 (0.01)	0.04 (0.05)
CU PACC-3[b]	−0.06 (0.20)	−0.09 (0.20)	−0.14 (0.25)
CI ADAS-Cog 11	1.30 (2.71)	1.61 (2.21)	3.11 (3.28)
Log CSF Aβ42/40 (1/y)	−0.0027 (0.0005)	−0.0027 (0.0007)	−0.0034 (0.0006)
Log CSF p-tau181, pg/mL/y	0.011 (0.013)	0.023 (0.022)	0.023 (0.017)

Abbreviations, ADAS-Cog 11, Alzheimer's Disease Assessment Scale–Cognitive Subscale; ADD, Alzheimer disease dementia; ADNI, Alzheimer's Disease Neuroimaging Initiative; APOE, apolipoprotein E; CI, cognitive impairment; CSF, cerebrospinal fluid; CU, cognitive unimpairment; FTP, [^{18}F]flortaucipir; HABS, Harvard Aging Brain Study; MCI, mild cognitive impairment; MMSE, Mini-Mental State Examination; p-tau181, tau phosphorylated at threonine 181; PACC-3, Preclinical Alzheimer Cognitive Composite; SUVR, standardized uptake value ratio.

[a] Only 915 participants had available APOE data (A^- $TMTL^-$, 241; A^- $TMTL^+$, 245; A^+ $TMTL^+$, 429).

[b] Sum of the *z* scores of the MMSE total score, Log-Transformed Trail Test B, and Logical Memory Delayed Recall.

To minimize the effect of subthreshold Aβ burden in the A^- $TMTL^+$ study group,[30-32] Aβ positivity was defined using a conservative cutoff of 12 centiloids.[27] This cut point proved to optimally discriminate between Thal phases 0 to 1 and 2 to 5[33] and it is therefore lower compared with traditional cut points based on discrimination of AD neuropathologic change levels (24.4 centiloids[33]) or reliable worsening (19 centiloids[34]). The tau-positivity threshold was defined as the 95th percentile of regional entorhinal cortex (ERC) SUVR values in the younger control cohort[34] (SUVR = 1.21) (eFigure 1 in Supplement 1).

CSF Biomarkers

Cerebrospinal fluid samples were collected for a subset of ADNI participants and processed according to previously described protocols.[35] Concentrations of Aβ1-42, Aβ1-40, and tau phosphorylated at threonine 181 (p-tau181) were measured by the ADNI Biomarker Core using the Roche Elecsys β-amyloid (1-42), β-amyloid(1-40), and phospho-tau (181P) CSF immunoassays. The CSF metrics used in this study included the baseline Aβ42/40 ratio (n = 359) and p-tau181 (n = 485) concentrations, as well as follow-up measurements for a subset of individuals (Aβ42/40: n = 77; mean [SD], 2.30 [1.03] years; p-tau181: n = 99; 2.34 [1.05] years).

Cognitive Assessments

Cognitive performance in cognitively unimpaired individuals was assessed using a modified version of the Preclinical Alzheimer Cognitive Composite[36] (PACC) derived as the sum of the *z* scores of the Mini-Mental State Examination total score, Log-Transformed Trail Test B, and Logical Memory Delayed Recall (PACC-3). The PACC-3 is designed to detect the first signs of cognitive decline in otherwise asymptomatic individuals. Cognitive performance in cognitively impaired individuals (combined mild cognitive impairment and AD dementia) was assessed using the Alzheimer's Disease Assessment Scale–Cognitive Subscale (ADAS-Cog 11).

Statistical Analysis

Statistical analysis of differences between the A^- $TMTL^-$ vs A^- $TMTL^+$ and A^+ $TMTL^+$ study groups was performed using generalized linear models (GLMs) controlled for age, sex, cohort (ADNI, HABS, and AVID-A05), and baseline centiloid values in the case of A^- $TMTL^+$ vs A^- $TMTL^-$ comparisons. Effect sizes were measured using Cohen *d*, and group differences between cortical maps were corrected for multiple comparisons using the FreeSurfer clusterwise correction for multiple comparisons. Longitudinal rates of change were computed using linear mixed-effect models with participant-specific intercepts and slopes (eg, V_k ~ time + (time|participant), where V_k is the value on the kth vertex of a cortical map).

First, we investigated vertex-wise and ROI-based group differences in baseline FTP SUVRs. Vertex and ROI-based group differences were also computed for the FTP SUVR longitudinal rates of change. Additionally, group differences in longitudinal centiloid accumulation were similarly investigated. Analysis of baseline and longitudinal differences in CSF Aβ42/40 and p-tau181 biomarker levels used analogous statistical models, but values were log-transformed before analysis to account for the exponential progression of CSF biomarker levels. Baseline and longitudinal differences across groups in cognitive metrics were studied separately for cognitively unimpaired and cognitively impaired individuals because of the different neuropsychological instruments that are best suited to detect the subtle cognitive changes in participants without impairment and more overt cognitive changes in those with impairment. As post hoc sensitivity analyses, we repeated the previous analyses with higher cut points for Aβ (24 centiloids) and tau PET positivity (mean +2.5 SD of the ERC FTP, SUVR = 1.27). Moreover, we assessed the outcome of using a larger MTL ROI comprising the ERC and amygdala.

In addition to the comparisons of dichotomized A and TMTL groups, complementary analyses were performed to assess continuous associations of baseline ERC FTP SUVR with vertex-wise cortical thickness patterns across all A^- individuals, using GLMs adjusted by sex, age, cohort, and baseline centiloid. Analogously, associations between baseline ERC FTP SUVR and cognitive performance were studied across the A^- subcohort with equally adjusted GLMs. Statistical tests were 2-sided, and $P < .05$ was considered statistically significant. The strength of the associations was assessed using the Pearson partial correlation coefficient (*r*).

Results

Demographic Characteristics

Of the 965 individuals included in the study, 462 were men (47.9%) and 503 were women (52.1%); mean (SD) age was 73.9 (8.1) years. A total of 51% A^- individuals and 78% of A^+ participants had increased tau PET signal in the ERC ($TMTL^+$) compared with healthy younger (age, <39 years) controls. Further demographic and biomarker characteristics are reported in the Table. Of participants with race data available (ie, ADNI and HABS cohorts), 92.9% of the individuals were White. Although no significant differences between women and men were found in baseline Braak stages I/II FTP-PET SUVR ($d = 0.10$; 95% CI, −0.02 to 0.23; $P = .10$) (eFigure 2 in Supplement 1), slightly higher longitudinal rates of Braak stages I/II FTP-PET SUVR change were observed in women ($d = 0.13$; 95% CI, 0.02-0.23; $P = .02$). Both A^- $TMTL^+$ (mean [SD] age, 74.9 [7.6] years; $d = 0.64$; 95% CI, 0.47-0.83; $P < .001$) and A^+ $TMTL^+$ (age, 75.6 [8.0] years; $d = 0.70$; 95% CI, 0.55-0.86, $P < .001$) individuals were significantly older than the A^- $TMTL^-$ control cohort (age, 70.0 [7.8] years). Similarly, both the A^+ $TMTL^+$ (60.4%; $d = 0.69$; 95% CI, 0.56-0.80; $P < .001$) and A^- $TMTL^+$ (33.7%; $d = 0.23$; 95% CI, 0.06-0.40; $P = .009$) groups had a significantly higher proportion of cognitively impaired individuals than the A^- $TMTL^-$ group (24.4%). The prevalence of apolipoprotein E (APOE)-ε4 was higher among A^+ $TMTL^+$ individuals (54.4%, $d = 0.64$; 95% CI, 0.54-0.76; $P < .001$), but was similar between the A^- $TMTL^+$ (18.0%; $d = -0.01$; 95% CI, −0.19 to 0.16; $P = .68$) and the A^- $TMTL^-$ control group (19.9%). By contrast, both the A^- $TMTL^-$ (16.3%) and A^- $TMTL^+$ groups (14.4%; $d = 0.08$; 95% CI, −0.10 to 0.25; $P = .38$) showed significantly higher proportions of APOE-ε2 carriers than the A^+ $TMTL^+$ group (4.4%; $d = 0.38$; 95% CI, 0.24-0.49; $P < .001$).

Tau and Aβ Accumulation

Analysis of baseline FTP SUVR contrast maps (**Figure 1**A) noted increased tau burden in A^- $TMTL^+$ individuals to be most pronounced in the MTL and extending into the inferior temporal lobe and the ventromedial prefrontal cortex, while A^+ $TMTL^+$ individuals showed the AD-characteristic pattern of widespread cortical tau accumulation across temporal, parietal, and frontal areas. In vertex-wise longitudinal FTP SUVR analyses, A^- $TMTL^-$ individuals showed little increase of tau accumulation over time, whereas the A^- $TMTL^+$ cohort displayed a moderate increase of tau uptake restricted to the MTL and inferior temporal regions (Figure 1B). By contrast, A^+ $TMTL^+$ participants showed a pronounced and widespread increase of tau accumulation. These differences were confirmed in direct statistical contrasts between the $TMTL^+$ groups and the A^- $TMTL^-$ group (Figure 1C). An ROI-based FTP SUVR analysis showcased similar results (eFigure 3 in Supplement 1), with A^- $TMTL^+$ participants showing statistically significant albeit moderate longitudinal (mean [SD], 1.83 [0.84] years) tau PET increases that were largely limited to the temporal lobe, whereas those with A^+ $TMTL^+$ showed faster and more cortically widespread tau PET increases.

Regarding Aβ accumulation, centiloid rates of change in A^- $TMTL^+$ participants did not show any significant increase in centiloids over time (mean [SD], 0.01 [12]; $P = .82$) (eFigure 4 in Supplement 1), although the slopes were slightly different from the slopes of the A^- $TMTL^-$ group (−0.17 [0.55]; $d = 0.29$; 95% CI, 0.04 to 0.54; $P = .04$) (Figure 1D). By contrast, A^+ $TMTL^+$ individuals showed a pronounced increase in centiloids over time (3.04 [1.98] vs −0.17 [0.55]; $d = 1.89$; 95% CI, 1.64 to 2.24; $P < .001$).

In the CSF subset analysis, A^- $TMTL^+$ participants showed moderately higher baseline p-tau181 levels compared with the A^- $TMTL^-$ group ($d = 0.24$; 95% CI, 0.002-0.48; $P = .04$), but no significant difference in Aβ42/40 ($d = -0.10$; 95% CI, −0.34

Figure 1. Cross-Sectional and Longitudinal Characterization of Amyloid-β (A) and Tau (T) Positron Emission Tomography Accumulation in the Medial Temporal Lobe (MTL)

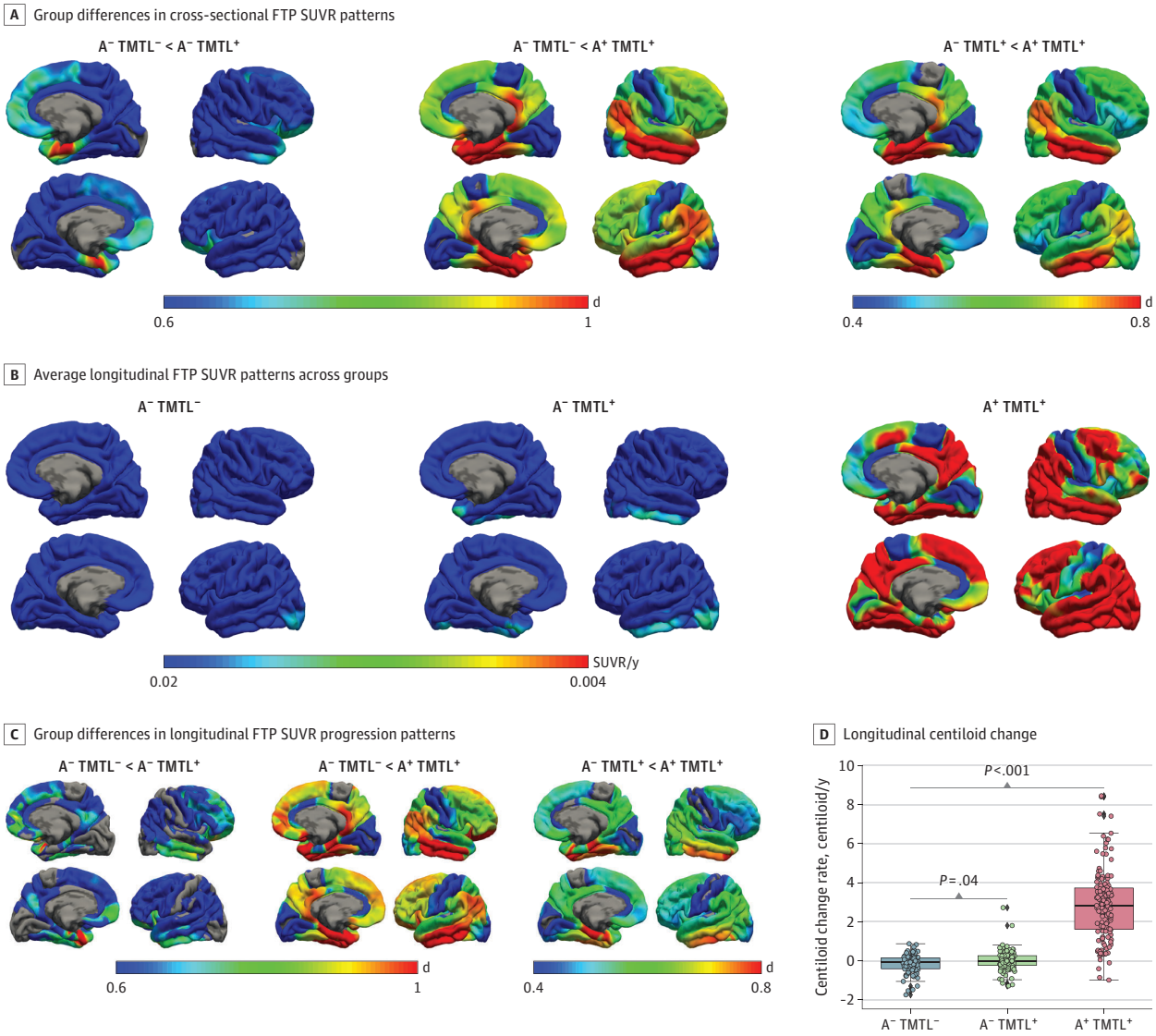

A, Vertex-wise group differences in cross-sectional [^{18}F]flortaucipir (FTP) standardized uptake value ratio (SUVR) patterns in A$^-$ TMTL$^+$ and A$^+$ TMTL$^+$ individuals compared with the control group, expressed as Cohen *d*. B, Average longitudinal FTP SUVR patterns in A$^-$ TMTL$^-$, A$^-$ TMTL$^+$, and A$^+$ TMTL$^+$ individuals, represented as vertex-wise rates of changes. C, Vertex-wise group differences in longitudinal FTP SUVR in A$^-$ TMTL$^+$ and A$^+$ TMTL$^+$ individuals compared with the A$^-$ TMTL$^-$ control group, expressed as Cohen *d*. D, Longitudinal centiloid change in A$^-$ TMTL$^-$, A$^-$ TMTL$^+$, and A$^+$ TMTL$^+$ individuals.

to 0.14; P = .38) (**Figure 2**A), whereas A$^+$ TMTL$^+$ individuals exhibited the expected alterations in both Aβ42/40 (d = −1.38; 95% CI, −1.66 to −1.14; P < .001) and p-tau181 (d = 1.00; 95% CI, 0.81-1.20; P < .001) levels (Figure 2A). In longitudinal analyses, the A$^-$ TMTL$^+$ group showed larger increases in p-tau181 levels over time at trend-level statistical significance (d = 0.52; 95% CI, 0.08-1.04; P = .07), but no significant difference in Aβ42/40 ratio change (d = 0.34; 95% CI, −0.16 to 0.94; P = .22), compared with the A$^-$ TMTL$^-$ group (Figure 2B). The A$^+$ TMTL$^+$ group showed significantly faster rates of change in both biomarkers (Aβ42/40: d = −1.33; 95% CI, −1.92 to −0.87; P < .001; p-tau181: d = 0.53; 95% CI, 0.07-1.06; P = .04).

Neurodegeneration

Compared with the A$^-$ TMTL$^-$ group, A$^-$ TMTL$^+$ participants (**Figure 3**A) showed cortical thinning at baseline mainly restricted to the MTL, whereas A$^+$ TMTL$^+$ participants showed more widespread cortical thinning extending to the lateral temporal lobe, the posterior cingulate, and the parietal and frontal lobes. This pattern was also reflected in ROI-based analyses, with A$^-$ TMTL$^+$ individuals showing significant cortical thinning in Braak stages I/II and Braak stages III/IV only (Figure 3B). The complementary analysis using continuous tau PET measures confirmed an association between ERC FTP SUVR and medial temporal neurodegeneration across A$^-$ individuals (eFigure 5 in Supplement 1).

Figure 2. Baseline and Longitudinal Characterization of Cerebrospinal Fluid (CSF) Amyloid-β (Aβ) and Tau Biomarkers

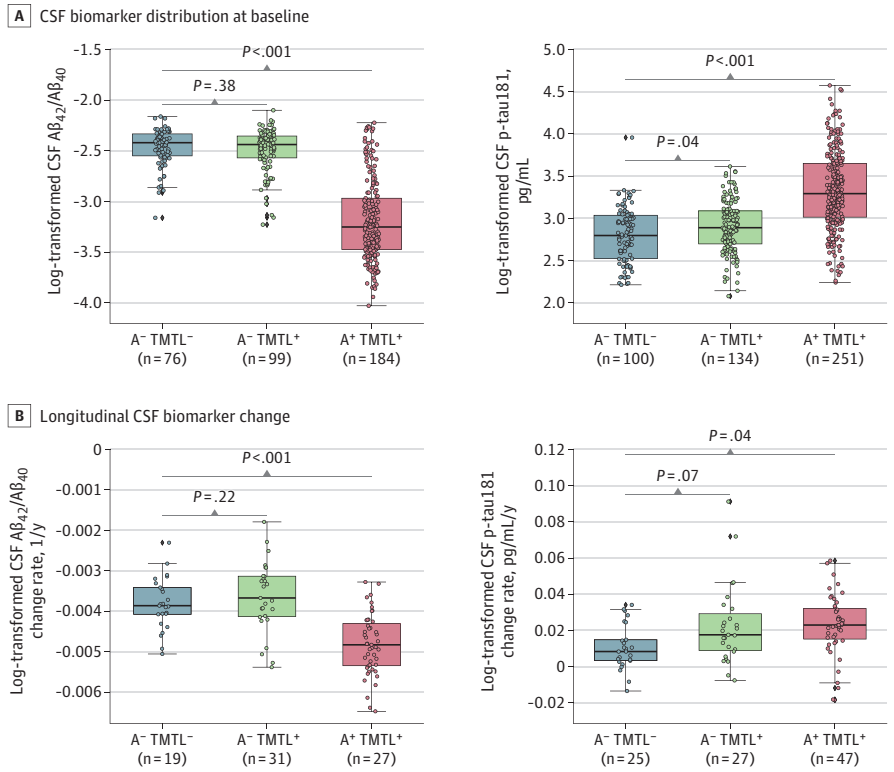

A, Baseline levels of CSF Aβ42/40 and tau phosphorylated at threonine 181 (p-tau181) across groups. Biomarker levels were statistically compared using generalized linear models (GLMs). B, Longitudinal change of CSF Aβ42/40 and p-tau181 metrics across groups, obtained using linear mixed-effect models and statistically compared with GLMs.

In longitudinal analyses, A⁻ TMTL⁺ individuals showed faster cortical thinning compared with the A⁻ TMTL⁻ group that was largely restricted to the MTL, while accelerated cortical thinning in the A⁺ TMTL⁺ group further extended to the lateral temporal, parietal, and frontal lobes (Figure 3C). Similarly, ROI-wise analyses (Figure 3D) showed significantly faster cortical thinning in A⁻ TMTL⁺ participants, mostly in Braak stages I/II.

Cognition

At baseline, cognitively impaired A⁺ TMTL⁺ individuals showed lower ADAS-Cog 11 scores compared with the cognitively impaired A⁻ TMTL⁻ group (d = −0.57; 95% CI, −0.79 to −0.34; P < .001), but neither the cognitively impaired A⁻ TMTL⁺ individuals nor any of the cognitively unimpaired groups differed significantly from the respective A⁻ TMTL⁻ controls (**Figure 4**). In the complementary analysis with continuous tau PET measures, baseline ERC FTP SUVR was significantly correlated with worse cognition in cognitively impaired A⁻ individuals (ADAS-Cog 11: r = 0.26; 95% CI, 0.08-0.46; P = .001), but not in cognitively unimpaired A⁻ individuals (PACC-3: r = 0.02; 95% CI, −0.09 to 0.13; P = .72).

Longitudinally, cognitively impaired individuals with A⁻ TMTL+ showed a comparable degree of moderate decline in ADAS-Cog 11 scores compared with cognitively impaired A⁻ TMTL⁻ individuals (d = 0.25; 95% CI, −0.11 to 0.58; P = .18), whereas cognitively impaired A⁺ TMTL⁺ participants showed significantly faster cognitive deterioration (d = 0.60; 95% CI, 0.30-0.90; P < .001) (eFigure 6 in Supplement 1). Among cognitively unimpaired participants, neither A⁻ TMTL⁺ (d = −0.06; 95% CI, −0.25 to 0.40; P = .61) nor A⁺ TMTL⁺ (d = −0.17; 95% CI, −0.44 to 0.14; P = .15) individuals showed a significant difference in PACC-3 decline compared with the A⁻ TMTL⁻ group. In the complementary analysis with continuous tau PET measures, baseline ERC FTP SUVR was significantly correlated with faster cognitive decline in cognitively impaired A⁻ individuals (ADAS-Cog 11: r = 0.30; 95% CI, 0.15-0.53; P < .001), but not in cognitively unimpaired A⁻ individuals (PACC-3: r = 0.03; 95% CI, −0.22 to 0.14; P = .63).

Sensitivity Analyses

Overall, the results derived from the sensitivity analyses were consistent with the main results presented in this study. Similar patterns of tau PET SUVR, CSF biomarkers, atrophy, and clinical change were found across the A TMTL groups when changing the Aβ PET cut point to 24 centiloids (eFigures 7-10 in Supplement 1) and when changing the Braak stages I/II SUVR cut point to 1.27 (eFigures 11-14 in the Supplement 1). Analyses using a larger MTL ROI (ERC plus amygdala) yielded a slightly different distribution of A TMTL groups (eFigure 15 in Supplement 1) and showed that the Aβ- and tau- accumulation patterns were similar to those obtained with the ERC ROI.

Figure 3. Baseline and Longitudinal Characterization of Atrophy, as Shown With Structural Magnetic Resonance Imaging

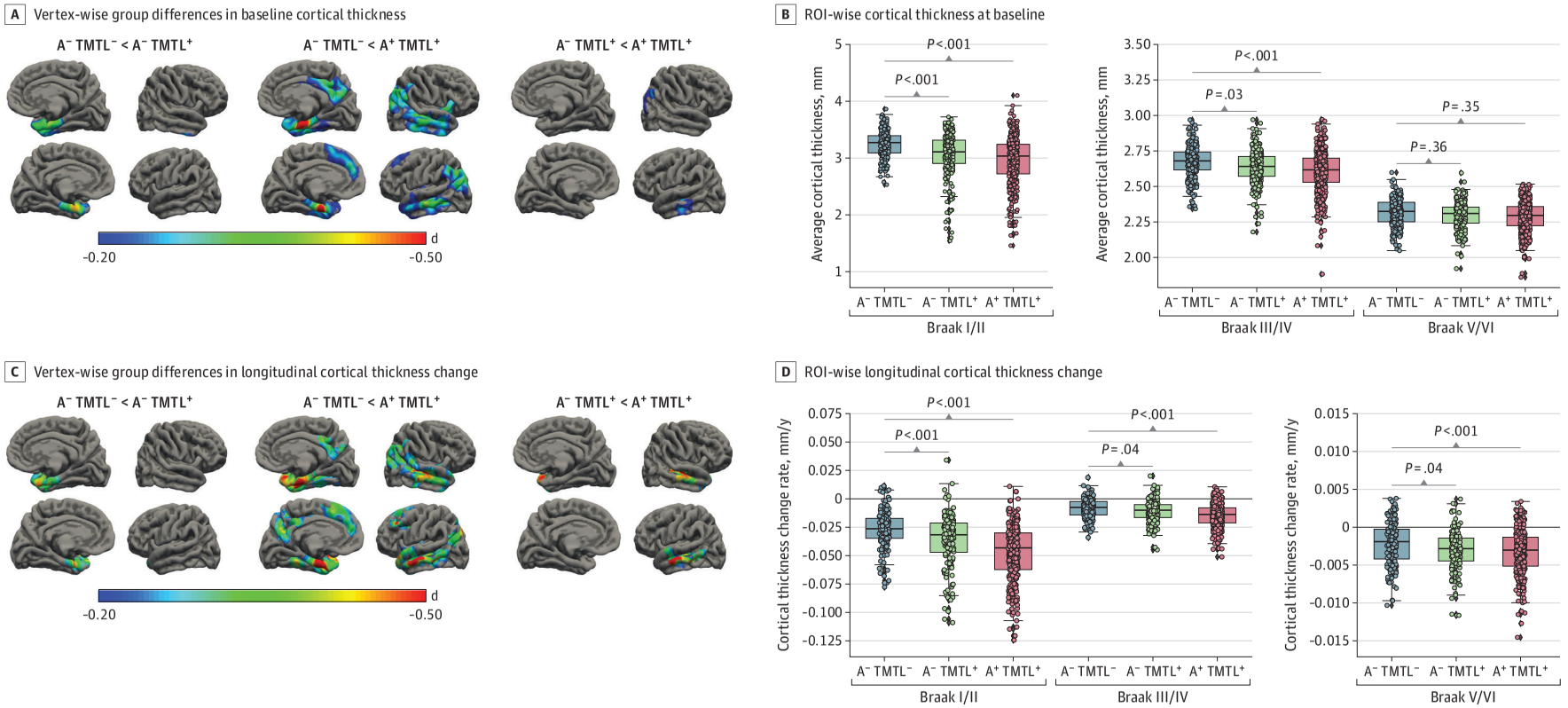

A, Vertex-wise group differences in baseline cortical thickness patterns in A^- $TMTL^+$ and A^+ $TMTL^+$ individuals compared with the A^- $TMTL^-$ control group, measured as Cohen *d*. B, Regional (region of interest [ROI]) group differences in baseline cortical thickness patterns in A^- $TMTL^+$ (Braak stages I/II: $d = -0.50$; 95% CI, −0.65 to −0.34; $P < .001$; Braak stages III/IV: $d = -0.20$; 95% CI, −0.38 to −0.02; $P = .025$; Braak stages V/VI: $d = -0.08$; 95% CI, −0.26 to 0.10; $P = .36$), and A^+ $TMTL^+$ individuals (Braak stages I/II: $d = -0.60$; 95% CI, −0.73 to −0.46; $P < .001$; Braak stages III/IV: $d = -0.34$; 95% CI, −0.49 to −0.20; $P < .001$; Braak stages V/VI: $d = -0.17$; 95% CI, −0.32 to −0.02; $P = .035$) compared with the A^- $TMTL^-$ control group using generalized linear models (GLM). C, Vertex-wise group differences in longitudinal cortical thickness progression patterns in A^- $TMTL^+$, and A^+ $TMTL^+$ individuals compared with the A^- $TMTL^-$ control group, measured as Cohen *d*. D, Regional group differences in longitudinal cortical thickness progression patterns in A^- $TMTL^+$ (Braak stages I/II: $d = -0.38$; 95% CI, −0.60 to −0.16; $P < .001$; Braak stages III/IV: $d = -0.22$; 95% CI, −0.44 to 0.008; $P = .044$; Braak stages V/VI: $d = -0.22$; 95% CI, −0.44 to −0.005; $P = .041$), and A^+ $TMTL^+$ individuals (Braak stages I/II: $d = -0.76$; 95% CI, −0.95 to −0.59; $P < .001$; Braak stages III/IV: $d = -0.57$; 95% CI, −0.76 to −0.39; $P < .001$; Braak stages V/VI: $d = -0.34$; 95% CI, −0.53 to −0.16; $P < .001$) compared with the A^- $TMTL^-$ control group using GLM models.

Figure 4. Baseline and Longitudinal Characterization of Cognitive Performance

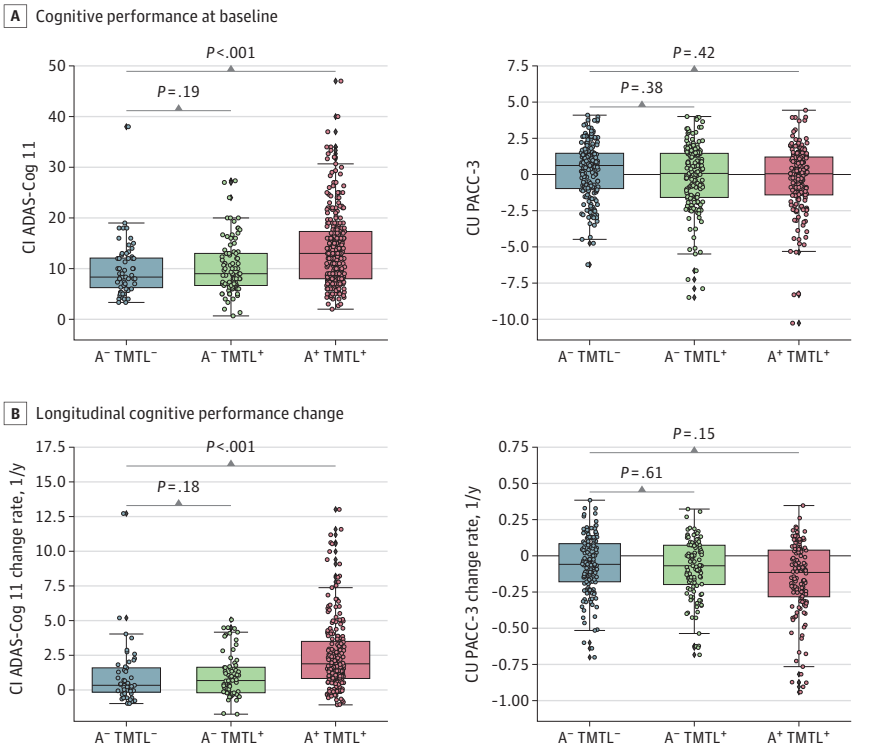

A, Baseline Alzheimer's Disease Assessment Scale–Cognitive Subscale (ADAS-Cog 11) scores in cognitively impaired (CI) individuals and sum of the *z* scores of the Mini-Mental State Examination total score, Log-Transformed Trail Test B, and Logical Memory Delayed Recall scores (PACC-3) in cognitively unimpaired (CU) individuals across amyloid-β (A) and tau (T) medial temporal lobe (MTL) groups, compared using generalized linear models (GLMs). B, Longitudinal changes in ADAS-Cog 11 scores in CI individuals and PACC-3 scores in CU individuals across A and TMTL groups, obtained with linear mixed-effect models and compared using GLMs.

Discussion

In this study, we explored in detail the pathologic and clinical course of older individuals who display PET-measured tau accumulation in the MTL in the absence of Aβ pathology (A^- $TMTL^+$), a condition reminiscent of pathologically defined PART.[5] In a large multicentric cohort of almost 1000 older individuals, we found that increased MTL tau PET signal without notable Aβ pathology is relatively common in older individuals and is associated with further longitudinal tau PET uptake increase, which remains largely restricted to the MTL. These tau PET increases colocalize with progressive MTL neurodegeneration, are associated with only subtle changes in global cognitive performance, and are not accompanied by notable accumulation of Aβ pathology over time.

Using a tau PET cutoff defined in healthy younger individuals, we observed that tau PET-measured MTL accumulation in the absence of Aβ is a common condition in older individuals, representing 51% of A^- individuals in this study. The frequency of tau PET positivity in this A^- sample is consistent with a previous study using a similar method (67%),[17] and it is substantially higher compared with previous studies using larger temporal ROIs without partial volume correction (approximately 17%-20%).[15,37] The discrepancy may be explained by use of extra-MTL ROIs without partial volume correction, which results in a lack of sensitivity to MTL-specific signal.

The degree to which FTP-PET can detect PART remains a subject of debate. PET-to-autopsy studies generally agree that local tau pathology needs to reach a certain density of neurofibrillary tangles to be detected in an FTP-PET scan, which is mostly the case for Braak stages V/VI.[38-41] This may lead to the conclusion that FTP-PET cannot detect PART-related tau deposition, which is, by definition, Braak stage IV or less. Yet, FTP showed binding to neurofibrillary tangles from PART brains in autoradiography studies[42,43] and, therefore, FTP-PET may detect a subset of PART cases with suprathreshold neurofibrillary tangle density. To date, the number of PART cases in the available PET-to-autopsy studies is low (n = 3)[38] and we cannot exclude that PART could be detected with FTP-PET in a subset of individuals. This hypothesis is consistent with the fact that the prevalence of tau PET positivity among older A^- individuals in our study (51%) is considerably lower than the prevalence of PART in this age range in neuropathologic studies.[5] The topography of our findings is also consistent with PART: in line with recent studies,[15,44,45] our results showed that increased tau PET signal in A^- $TMTL^+$ individuals was largely limited to the MTL. Both baseline and longitudinal increases in tau PET signal in A^- $TMTL^+$ individuals were found to be paralleled by increases in CSF p-tau181 levels, suggesting that these signal increases reflect actual increases in tau burden. Together, these results suggest that PART may be an important neuropathologic substrate for many A^- $TMTL^+$ individuals in our study, although probably not the only one.[15]

We also acknowledge that pathologic entities other than PART may lead to abnormal FTP-PET signal in the MTL among Aβ-negative individuals. Although FTP shows high specificity for AD-type tau aggregates in autoradiography studies,[42,46,47] extensive increases in cortical FTP-PET signal

in the absence of Aβ can occur in patients with AD dementia or mild cognitive impairment, which likely represent tangle-predominant dementia.[15,48] Moreover, FTP-PET increases can occur in frontotemporal dementia syndromes, including those associated with tau and TAR DNA-binding protein 43 (TDP-43).[49-52] The binding mechanisms remain unclear, although binding to non-AD tau as well as to neurodegenerative processes that colocalize with TDP-43 deposition might result in nonspecific FTP binding.[49,53] Therefore, we cannot exclude the possibility that limbic-predominant age-related TDP-43 encephalopathy, which is associated with neurodegeneration in the MTL, might also result in abnormal FTP-PET signal in the same regions, although the influence of limbic-predominant age-related TDP-43 encephalopathy on FTP-PET appears to be limited.[54] These considerations suggest that the A^- $TMTL^+$ group likely represents both a clinically and pathologically heterogeneous group. Thus, increased FTP-PET signal in the MTL in the absence of Aβ should not be considered a specific marker of PART. Despite these limitations, our findings are valuable and contribute to understanding the clinical and pathologic course of the A^- $TMTL^+$ group as a whole. Yet, given its high frequency among cognitively unimpaired individuals and those with mild average cognitive decline, the clinical significance of the A^- $TMTL^+$ profile remains uncertain. Additional work is needed to identify the subset of A^- $TMTL^+$ individuals who will experience more relevant clinical outcomes.

Given that longitudinal follow-up of neuropathologically defined PART is not possible, a main controversy exists whether PART reflects an early form of AD, with Aβ pathology developing in the further disease course, or whether it represents an entirely distinct pathologic entity.[12-14] Herein, we noted that A^- $TMTL^+$ individuals did not show significant Aβ accumulation over the available follow-up period, thus arguing against the possibility that this condition reflects an early tau-first subtype of AD.[55]

Longitudinal cortical thickness analysis demonstrated that A^- $TMTL^+$ individuals have moderate and restricted MTL atrophy progression, whereas atrophy is more accelerated and spreads to widespread neocortical regions in A^+ $TMTL^+$ participants. These results suggest that tau accumulation in Aβ-negative individuals is not a benign process but is associated with increased neurodegeneration,[56] although the rates of progression are significantly slower compared with rates in A^+ $TMTL^+$ participants.

In cognition analyses, we did not find significant differences in baseline performance or longitudinal decline between A^- $TMTL^+$ individuals and the A^- $TMTL^-$ controls, whereas a significantly faster decline was observed in cognitively impaired A^+ $TMTL^+$ individuals. However, a more sensitive analysis using continuous tau measures showed an association of ERC tau uptake with worse cognition and faster cognitive decline also in cognitively impaired A^- participants. These results suggest that, in the absence of Aβ, tau accumulation in the MTL has only subtle effects on cognition and does not herald the pronounced cognitive decline typical for AD. Further research with longer follow-up might be necessary to delineate the long-term consequences of ongoing tau accumulation in the absence of Aβ.

Limitations

This study has limitations. The first of these is the lack of autopsy data of A^- $TMTL^+$ individuals, which leaves the exact association between the PET-defined A^- $TMTL^+$ group and PART to be determined. Second, we relied on cutoffs for group definition. While centiloid cutoffs for denoting Aβ status are well established,[27] a number of different methods and cutoffs for defining tau PET positivity have been used in the literature, resulting in highly variable proportions of the different A and TMTL groups.[57] Herein, we applied a commonly used method for objectively defining biomarker cutoffs based on data from healthy younger controls,[34] and several of our principal findings were replicated in complementary continuous analyses that are independent of cutoff definition. Third, to achieve robust sample sizes of the less-prevalent A^- $TMTL^+$ individuals, we pooled data across different cohorts. While the possible influence of multicentric data acquisitions was minimized by harmonizing imaging preprocessing, it limited our ability to analyze domain-specific cognitive decline, as neuropsychological instruments differed across cohorts. Fourth, follow-up time for the evaluation of both longitudinal clinical and biomarker measures was relatively short. Fifth, the cohorts included in our study represent selective research cohorts that may not reflect the general population, and our findings should be replicated in more diverse cohorts.

Conclusions

The results presented in this longitudinal cohort study suggest that individuals with MTL tau accumulation in the absence of Aβ follow a separate, less malign, pathologic course compared with that of typical AD. While these individuals showed progressive tau accumulation and neurodegeneration, this process was comparably slow, remained largely restricted to the MTL, and was associated with only subtle changes in global cognitive performance. Moreover, these individuals did not show notable Aβ accumulation over follow-up, arguing against the possibility that this A^- $TMTL^+$ condition reflects a tau-first subtype of AD. Further studies are warranted that specify the exact association of this common PET-defined condition with pathologic PART.

ARTICLE INFORMATION

Accepted for Publication: May 16, 2023.

Published Online: August 14, 2023. doi:10.1001/jamaneurol.2023.2560

Author Affiliations: Universidade de Santiago de Compostela, Santiago de Compostela, Spain (Costoya-Sánchez, Aguiar); Nuclear Medicine Department and Molecular Imaging Group, Instituto de Investigación Sanitaria de Santiago de Compostel, Travesía da Choupana s/n, Santiago de Compostela, Spain (Costoya-Sánchez, Aguiar); Centro de Investigación Biomédica en Red sobre Enfermedades Neurodegenerativas, Instituto de

Salud Carlos III, Madrid, Spain (Costoya-Sánchez, Silva-Rodríguez, Aguiar, Grothe); Wallenberg Centre for Molecular and Translational Medicine, University of Gothenburg, Gothenburg, Sweden (Moscoso, Schöll, Grothe); Department of Psychiatry and Neurochemistry, Institute of Physiology and Neuroscience, University of Gothenburg, Gothenburg, Sweden (Moscoso, Schöll); Unidad de Trastornos del Movimiento, Servicio de Neurología y Neurofisiología Clínica, Instituto de Biomedicina de Sevilla, Hospital Universitario Virgen del Rocío/CSIC/Universidad de Sevilla, Seville, Spain (Silva-Rodríguez, Grothe); Avid Radiopharmaceuticals, Philadelphia, Pennsylvania (Pontecorvo, Devous); Eli Lilly and Company, Indianapolis, Indiana (Pontecorvo, Devous); Dementia Research Centre, Institute of Neurology, University College London, London, United Kingdom (Schöll).

Author Contributions: Mr Costoya-Sánchez and Dr Moscoso contributed equally to the study, had full access to all of the data in the study, and take responsibility for the integrity of the data and the accuracy of the data analysis. Equally contributing last authors: Drs Aguiar, Schöll, and Grothe.
Concept and design: Costoya-Sánchez, Moscoso, Devous, Schöll, Grothe.
Acquisition, analysis, or interpretation of data: All authors.
Drafting of the manuscript: Costoya-Sánchez, Moscoso, Aguiar, Grothe.
Statistical analysis: Costoya-Sánchez, Moscoso, Grothe.
Obtained funding: Aguiar, Schöll.
Administrative, technical, or material support: Silva-Rodríguez, Aguiar.
Supervision: Moscoso, Silva-Rodríguez, Devous, Aguiar, Schöll, Grothe.

Conflict of Interest Disclosures: Dr Silva-Rodríguez reported that he is a founder and advisor for Qubiotech Health Intelligence SL, a company commercializing neuroimaging quantification software. Dr Pontecorvo reported being an Eli Lilly and Company employee and minor stockholder outside the submitted work. Dr Devous reported being an Eli Lilly and Company employee and minor stockholder outside the submitted work. Dr Aguiar reported being a cofounder of Qubiotech Health Intelligence SL. Dr Schöll has served on advisory boards for Roche and Novo Nordisk (outside scope of submitted work). No other disclosures were reported.

Funding/Support: We thank AVID Radiopharmaceuticals for supporting this study by facilitating access to the AVID-A05 data. The project that gave rise to these results received the support of a fellowship from la Caixa Foundation (ID 100010434). The fellowship code is LCF/BQ/DR20/11790012. Dr Aguiar and Mr Costoya-Sánchez are supported by the research grant PI19/01315 of the Instituto de Salud Carlos III-Fondo Europeo de Desarrollo Regional (ISCIII-FEDER) and by the Centro de Investigaciones Biomédicas en Red (CIBER, CB22/05/00067). Dr Grothe is supported by the Miguel Servet program (CP19/00031) and research grant PI20/00613 of the ISCIII-FEDER. Dr. Silva-Rodríguez is supported by the "Sara Borrell" program (CD21/00067) of the ISCIII-FEDER. Dr Schöll is supported by the Knut and Alice Wallenberg Foundation (Wallenberg Centre for Molecular and Translational Medicine; KAW2014.0363 and KAW 2023.0371), the Swedish Research Council (2017-02869, 2021-02678 and 2021-06545), the European Union's Horizon Europe research and innovation program under grant agreement no 101132933 (AD-RIDDLE), the National Institute of Health (R01 AG081394-01), the Swedish state under the agreement between the Swedish government and the County Councils, the ALF-agreement (ALFGBG-813971 and ALFGBG-965326), the Swedish Brain Foundation (FO2021-0311) and the Swedish Alzheimer Foundation (AF-740191). Data collection and sharing for this project was funded by the Alzheimer's Disease Neuroimaging Initiative (ADNI) (National Institutes of Health grant U01 AG024904) and Department of Defense ADNI (award W81XWH-12-2-0012). The ADNI is funded by the National Institute on Aging, and the National Institute of Biomedical Imaging and Bioengineering, and through generous contributions from the following: AbbVie, Alzheimer's Association, Alzheimer's Drug Discovery Foundation, Araclon Biotech, BioClinica Inc, Biogen, Bristol-Myers Squibb Company, CereSpir Inc, Cogstate, Eisai Inc, Elan Pharmaceuticals Inc, Eli Lilly and Company, EuroImmun, F. Hoffmann-La Roche Ltd and its affiliated company Genentech Inc, Fujirebio, GE Healthcare, IXICO Ltd, Janssen Alzheimer Immunotherapy Research & Development LLC, Johnson & Johnson Pharmaceutical Research & Development LLC, Lumosity, Lundbeck, Merck & Co Inc, Meso Scale Diagnostics LLC, NeuroRx Research, Neurotrack Technologies, Novartis Pharmaceuticals Corp, Pfizer Inc, Piramal Imaging, Servier, Takeda Pharmaceutical Company, and Transition Therapeutics. The Canadian Institutes of Health Research is providing funds to support ADNI clinical sites in Canada. Private sector contributions are facilitated by the Foundation for the National Institutes of Health (www.fnih.org). The grantee organization is the Northern California Institute for Research and Education, and the study is coordinated by the Alzheimer's Therapeutic Research Institute at the University of Southern California.

Role of the Funder/Sponsor: The funding organizations had no role in the design and conduct of the study; collection, management, analysis, and interpretation of the data; preparation, review, or approval of the manuscript; and decision to submit the manuscript for publication.

Group Information: Members of the Alzheimer's Disease Neuroimaging Initiative and the Harvard Aging Brain Study appear in Supplement 2.

Data Sharing Statement: See Supplement 3.

Additional Information: Part of the data used in preparation of this article were obtained from the Alzheimer's Disease Neuroimaging Initiative (ADNI) database (adni.loni.usc.edu). As such, the investigators within the ADNI contributed to the design and implementation of ADNI and/or provided data but did not participate in the analysis or the writing of this report. A complete listing of ADNI investigators can be found at https://adni.loni.usc.edu/wp-content/uploads/how_to_apply/ADNI_Acknowledgement_List.pdf.pdf . Part of the data used in the preparation of this article were obtained from the Harvard Aging Brain Study (HABS-P01AG036694; https://habs.mgh.harvard.edu). The HABS study was launched in 2010, funded by the National Institute on Aging, and is led by principal investigators Reisa A. Sperling, MD, and Keith A. Johnson, MD, at Massachusetts General Hospital/Harvard Medical School, Boston. Dr Devous retired.

REFERENCES

1. Duyckaerts C, Delatour B, Potier M-C. Classification and basic pathology of Alzheimer disease. *Acta Neuropathol*. 2009;118(1):5-36. doi:10.1007/s00401-009-0532-1

2. Serrano-Pozo A, Frosch MP, Masliah E, Hyman BT. Neuropathological alterations in Alzheimer disease. *Cold Spring Harb Perspect Med*. 2011;1(1):a006189-a006189. doi:10.1101/cshperspect.a006189

3. Bennett DA, Schneider JA, Wilson RS, Bienias JL, Arnold SE. Neurofibrillary tangles mediate the association of amyloid load with clinical Alzheimer disease and level of cognitive function. *Arch Neurol*. 2004;61(3):378-384. doi:10.1001/archneur.61.3.378

4. Braak H, Thal DR, Ghebremedhin E, Del Tredici K. Stages of the pathologic process in Alzheimer disease: age categories from 1 to 100 years. *J Neuropathol Exp Neurol*. 2011;70(11):960-969. doi:10.1097/NEN.0b013e318232a379

5. Crary JF, Trojanowski JQ, Schneider JA, et al. Primary age-related tauopathy (PART): a common pathology associated with human aging. *Acta Neuropathol*. 2014;128(6):755-766. doi:10.1007/s00401-014-1349-0

6. Josephs KA, Murray ME, Tosakulwong N, et al. Tau aggregation influences cognition and hippocampal atrophy in the absence of beta-amyloid: a clinico-imaging-pathological study of primary age-related tauopathy (PART). *Acta Neuropathol*. 2017;133(5):705-715. doi:10.1007/s00401-017-1681-2

7. Besser LM, Crary JF, Mock C, Kukull WA. Comparison of symptomatic and asymptomatic persons with primary age-related tauopathy. *Neurology*. 2017;89(16):1707-1715. doi:10.1212/WNL.0000000000004521

8. Jefferson-George KS, Wolk DA, Lee EB, McMillan CT. Cognitive decline associated with pathological burden in primary age-related tauopathy. *Alzheimers Dement*. 2017;13(9):1048-1053. doi:10.1016/j.jalz.2017.01.028

9. Bell WR, An Y, Kageyama Y, et al. Neuropathologic, genetic, and longitudinal cognitive profiles in primary age-related tauopathy (PART) and Alzheimer's disease. *Alzheimers Dement*. 2019;15(1):8-16. doi:10.1016/j.jalz.2018.07.215

10. Besser LM, Mock C, Teylan MA, Hassenstab J, Kukull WA, Crary JF. Differences in cognitive impairment in primary age-related tauopathy versus Alzheimer disease. *J Neuropathol Exp Neurol*. 2019;78(3):219-228. doi:10.1093/jnen/nly132

11. Jack CR Jr, Bennett DA, Blennow K, et al; Contributors. NIA-AA Research Framework: toward a biological definition of Alzheimer's disease. *Alzheimers Dement*. 2018;14(4):535-562. doi:10.1016/j.jalz.2018.02.018

12. Duyckaerts C, Braak H, Brion JP, et al. PART is part of Alzheimer disease. *Acta Neuropathol*. 2015;129(5):749-756. doi:10.1007/s00401-015-1390-7

13. Jellinger KA, Alafuzoff I, Attems J, et al. PART, a distinct tauopathy, different from classical sporadic Alzheimer disease. *Acta Neuropathol*. 2015;129(5):757-762. doi:10.1007/s00401-015-1407-2

14. Jack CR Jr. PART and SNAP. *Acta Neuropathol*. 2014;128(6):773-776. doi:10.1007/s00401-014-1362-3

15. Yoon B, Guo T, Provost K, et al; Alzheimer's Disease Neuroimaging Initiative. Abnormal tau in

amyloid PET negative individuals. *Neurobiol Aging*. 2022;109:125-134. doi:10.1016/j.neurobiolaging.2021.09.019

16. Altomare D, Caprioglio C, Assal F, et al. Diagnostic value of amyloid-PET and tau-PET: a head-to-head comparison. *Eur J Nucl Med Mol Imaging*. 2021;48(7):2200-2211. doi:10.1007/s00259-021-05246-x

17. Weigand AJ, Bangen KJ, Thomas KR, et al; Alzheimer's Disease Neuroimaging Initiative. Is tau in the absence of amyloid on the Alzheimer's continuum? a study of discordant PET positivity. *Brain Commun*. 2020;2(1):fcz046. doi:10.1093/braincomms/fcz046

18. Jagust WJ, Landau SM, Shaw LM, et al; Alzheimer's Disease Neuroimaging Initiative. Relationships between biomarkers in aging and dementia. *Neurology*. 2009;73(15):1193-1199. doi:10.1212/WNL.0b013e3181bc010c

19. Dagley A, LaPoint M, Huijbers W, et al. Harvard Aging Brain Study: dataset and accessibility. *Neuroimage*. 2017;144(pt B):255-258. doi:10.1016/j.neuroimage.2015.03.069

20. Braak H, Alafuzoff I, Arzberger T, Kretzschmar H, Del Tredici K. Staging of Alzheimer disease–associated neurofibrillary pathology using paraffin sections and immunocytochemistry. *Acta Neuropathol*. 2006;112(4):389-404. doi:10.1007/s00401-006-0127-z

21. Biel D, Brendel M, Rubinski A, et al; Alzheimer's Disease Neuroimaging Initiative (ADNI). Tau-PET and in vivo Braak-staging as prognostic markers of future cognitive decline in cognitively normal to demented individuals. *Alzheimers Res Ther*. 2021;13(1):137. doi:10.1186/s13195-021-00880-x

22. Jagust WJ, Bandy D, Chen K, et al; Alzheimer's Disease Neuroimaging Initiative. The Alzheimer's Disease Neuroimaging Initiative positron emission tomography core. *Alzheimers Dement*. 2010;6(3):221-229. doi:10.1016/j.jalz.2010.03.003

23. López-González FJ, Costoya-Sánchez A, Paredes-Pacheco J, Moscoso A, Silva-Rodríguez J, Aguiar P; Alzheimer's Disease Neuroimaging Initiative. Impact of spill-in counts from off-target regions on [^{18}F]flortaucipir PET quantification. *Neuroimage*. 2022;259:119396. doi:10.1016/j.neuroimage.2022.119396

24. Thomas BA, Erlandsson K, Modat M, et al. The importance of appropriate partial volume correction for PET quantification in Alzheimer's disease. *Eur J Nucl Med Mol Imaging*. 2011;38(6):1104-1119. doi:10.1007/s00259-011-1745-9

25. Thomas BA, Cuplov V, Bousse A, et al. PETPVC: a toolbox for performing partial volume correction techniques in positron emission tomography. *Phys Med Biol*. 2016;61(22):7975-7993. doi:10.1088/0031-9155/61/22/7975

26. Baker SL, Maass A, Jagust WJ. Considerations and code for partial volume correcting [^{18}F]-AV-1451 tau PET data. *Data Brief*. 2017;15:648-657. doi:10.1016/j.dib.2017.10.024

27. Klunk WE, Koeppe RA, Price JC, et al. The Centiloid Project: standardizing quantitative amyloid plaque estimation by PET. *Alzheimers Dement*. 2015;11(1):1-15.e1, 4. doi:10.1016/j.jalz.2014.07.003

28. Dale AM, Fischl B, Sereno MI. Cortical surface-based analysis, I: segmentation and surface reconstruction. *Neuroimage*. 1999;9(2):179-194. doi:10.1006/nimg.1998.0395

29. Fischl B, Sereno MI, Dale AM. Cortical surface-based analysis, II: inflation, flattening, and a surface-based coordinate system. *Neuroimage*. 1999;9(2):195-207. doi:10.1006/nimg.1998.0396

30. Diedrichsen J. A spatially unbiased atlas template of the human cerebellum. *Neuroimage*. 2006;33(1):127-138. doi:10.1016/j.neuroimage.2006.05.056

31. Mormino EC, Insel PS. Uncertainties in the PET defined A-/$T_{Neocortical}$+ subtype. *Alzheimers Dement (Amst)*. 2022;14(1):e12348.

32. Krishnadas N, Doré V, Laws SM, et al. Exploring discordant low amyloid beta and high neocortical tau positron emission tomography cases. *Alzheimers Dement (Amst)*. 2022;14(1):e12326. doi:10.1002/dad2.12326

33. La Joie R, Ayakta N, Seeley WW, et al. Multisite study of the relationships between antemortem [^{11}C]PIB-PET centiloid values and postmortem measures of Alzheimer's disease neuropathology. *Alzheimers Dement*. 2019;15(2):205-216. doi:10.1016/j.jalz.2018.09.001

34. Jack CR Jr, Wiste HJ, Weigand SD, et al. Defining imaging biomarker cut points for brain aging and Alzheimer's disease. *Alzheimers Dement*. 2017;13(3):205-216. doi:10.1016/j.jalz.2016.08.005

35. Kang JH, Korecka M, Figurski MJ, et al; Alzheimer's Disease Neuroimaging Initiative. The Alzheimer's Disease Neuroimaging Initiative 2 Biomarker Core: a review of progress and plans. *Alzheimers Dement*. 2015;11(7):772-791. doi:10.1016/j.jalz.2015.05.003

36. Donohue MC, Sperling RA, Salmon DP, et al; Australian Imaging, Biomarkers, and Lifestyle Flagship Study of Ageing; Alzheimer's Disease Neuroimaging Initiative; Alzheimer's Disease Cooperative Study. The preclinical Alzheimer cognitive composite: measuring amyloid-related decline. *JAMA Neurol*. 2014;71(8):961-970. doi:10.1001/jamaneurol.2014.803

37. Jack CR Jr, Wiste HJ, Weigand SD, et al. Age-specific and sex-specific prevalence of cerebral β-amyloidosis, tauopathy, and neurodegeneration in cognitively unimpaired individuals aged 50-95 years: a cross-sectional study. *Lancet Neurol*. 2017;16(6):435-444. doi:10.1016/S1474-4422(17)30077-7

38. Lowe VJ, Lundt ES, Albertson SM, et al. Tau-positron emission tomography correlates with neuropathology findings. *Alzheimers Dement*. 2020;16(3):561-571. doi:10.1016/j.jalz.2019.09.079

39. Fleisher AS, Pontecorvo MJ, Devous MD Sr, et al; A16 Study Investigators. Positron emission tomography imaging with [18F]flortaucipir and postmortem assessment of Alzheimer disease neuropathologic changes. *JAMA Neurol*. 2020;77(7):829-839. doi:10.1001/jamaneurol.2020.0528

40. Moscoso A, Wren MC, Lashley T, et al. Imaging tau pathology in Alzheimer's disease with positron emission tomography: lessons learned from imaging-neuropathology validation studies. *Mol Neurodegener*. 2022;17(1):39. doi:10.1186/s13024-022-00543-x

41. Soleimani-Meigooni DN, Iaccarino L, La Joie R, et al. 18F-flortaucipir PET to autopsy comparisons in Alzheimer's disease and other neurodegenerative diseases. *Brain*. 2020;143(11):3477-3494. doi:10.1093/brain/awaa276

42. Lowe VJ, Curran G, Fang P, et al. An autoradiographic evaluation of AV-1451 Tau PET in dementia. *Acta Neuropathol Commun*. 2016;4(1):58. doi:10.1186/s40478-016-0315-6

43. Marquié M, Siao Tick Chong M, Antón-Fernández A, et al. [F-18]-AV-1451 binding correlates with postmortem neurofibrillary tangle Braak staging. *Acta Neuropathol*. 2017;134(4):619-628. doi:10.1007/s00401-017-1740-8

44. Groot C, Doré V, Robertson J, et al. Mesial temporal tau is related to worse cognitive performance and greater neocortical tau load in amyloid-β–negative cognitively normal individuals. *Neurobiol Aging*. 2021;97:41-48. doi:10.1016/j.neurobiolaging.2020.09.017

45. Krishnadas N, Doré V, Groot C, et al; AIBL research group. Mesial temporal tau in amyloid-β–negative cognitively normal older persons. *Alzheimers Res Ther*. 2022;14(1):51. doi:10.1186/s13195-022-00993-x

46. Marquié M, Normandin MD, Vanderburg CR, et al. Validating novel tau positron emission tomography tracer [F-18]-AV-1451 (T807) on postmortem brain tissue. *Ann Neurol*. 2015;78(5):787-800. doi:10.1002/ana.24517

47. Marquié M, Normandin MD, Meltzer AC, et al. Pathological correlations of [F-18]-AV-1451 imaging in non-Alzheimer tauopathies. *Ann Neurol*. 2017;81(1):117-128. doi:10.1002/ana.24844

48. Serrano-Pozo A, Qian J, Monsell SE, et al. Mild to moderate Alzheimer dementia with insufficient neuropathological changes. *Ann Neurol*. 2014;75(4):597-601. doi:10.1002/ana.24125

49. Tsai RM, Bejanin A, Lesman-Segev O, et al. ^{18}F-flortaucipir (AV-1451) tau PET in frontotemporal dementia syndromes. *Alzheimers Res Ther*. 2019;11(1):13. doi:10.1186/s13195-019-0470-7

50. Makaretz SJ, Quimby M, Collins J, et al. Flortaucipir tau PET imaging in semantic variant primary progressive aphasia. *J Neurol Neurosurg Psychiatry*. 2018;89(10):1024-1031. doi:10.1136/jnnp-2017-316409

51. Josephs KA, Martin PR, Botha H, et al. [^{18} F]AV-1451 tau-PET and primary progressive aphasia. *Ann Neurol*. 2018;83(3):599-611. doi:10.1002/ana.25183

52. Wolters EE, Papma JM, Verfaillie SCJ, et al. [^{18}F]flortaucipir PET across various *MAPT* mutations in presymptomatic and symptomatic carriers. *Neurology*. 2021;97(10):e1017-e1030. doi:10.1212/WNL.0000000000012448

53. Schaeverbeke J, Celen S, Cornelis J, et al. Binding of [^{18}F]AV1451 in post mortem brain slices of semantic variant primary progressive aphasia patients. *Eur J Nucl Med Mol Imaging*. 2020;47(8):1949-1960. doi:10.1007/s00259-019-04631-x

54. Carlos AF, Tosakulwong N, Weigand SD, et al. TDP-43 pathology effect on volume and flortaucipir uptake in Alzheimer's disease. *Alzheimers Dement*. 2023;19(6):2343-2354. doi:10.1002/alz.12878

55. Aksman LM, Oxtoby NP, Scelsi MA, et al. Tau-first subtype of Alzheimer's disease consistently identified across in vivo and post mortem studies. *bioRxiv*. Preprint posted online December 19, 2020. doi:10.1101/2020.12.18.418004

56. Das SR, Xie L, Wisse LEM, et al; Alzheimer's Disease Neuroimaging Initiative. In vivo measures of tau burden are associated with atrophy in early Braak stage medial temporal lobe regions in amyloid-negative individuals. *Alzheimers Dement*. 2019;15(10):1286-1295. doi:10.1016/j.jalz.2019.05.009

57. Weigand AJ, Maass A, Eglit GL, Bondi MW. What's the cut-point? a systematic investigation of tau PET thresholding methods. *Alzheimers Res Ther*. 2022;14(1):49. doi:10.1186/s13195-022-00986-w